Biochem. J. (2014) **457**, 323–334 (Printed in Great Britain) doi:10.1042/BJ20131174

A robust methodology to subclassify pseudokinases based on their nucleotide-binding properties

James M. MURPHY*†[1,2], Qingwei ZHANG‡, Samuel N. YOUNG*, Michael L. REESE§[3], Fiona P. BAILEY¶, Patrick A. EYERS¶, Daniela UNGUREANU‖, Henrik HAMMAREN‖, Olli SILVENNOINEN‖, Leila N. VARGHESE*†, Kelan CHEN*†, Anne TRIPAYDONIS*, Natalia JURA**, Koichi FUKUDA††, Jun QIN††, Zachary NIMCHUK‡‡[4], Mary Beth MUDGETT§§, Sabine ELOWE¶¶, Christine L. GEE‖‖, Ling LIU***[5], Roger J. DALY***[5], Gerard MANNING†††, Jeffrey J. BABON*† and Isabelle S. LUCET‡[1,2]

*The Walter and Eliza Hall Institute of Medical Research, Parkville, Victoria 3052, Australia
†Department of Medical Biology, University of Melbourne, Parkville, Victoria 3050, Australia
‡Department of Biochemistry and Molecular Biology, School of Biomedical Sciences, Monash University, Clayton, Victoria 3800, Australia
§Department of Microbiology and Immunology, Stanford University, Stanford, CA 24305-5124, U.S.A.
¶Department of Biochemistry, Institute of Integrative Biology, University of Liverpool, Liverpool L69 7ZB, U.K.
‖School of Medicine and Institute of Biomedical Technology, University of Tampere and Tampere University Hospital, Tampere 33014, Finland
**Cardiovascular Research Institute and Department of Cellular and Molecular Pharmacology, University of California San Francisco, San Francisco, CA 94158-9001, U.S.A.
††Department of Molecular Cardiology, Lerner Research Institute, NB20, Cleveland Clinic, 9500 Euclid Avenue, Cleveland, OH 44195, U.S.A.
‡‡Department of Biology, California Institute of Technology, Pasadena, CA 91125, U.S.A.
§§Department of Biology, Stanford University, Stanford, CA 24305-5020, U.S.A.
¶¶Centre de Recherche du Centre Hospitalier Universitaire de Québec and and Faculté de Médicine, Département de Pédiatrie, Université Laval, Québec G1V 4G2, Canada
‖‖Australian Synchrotron, Clayton, Victoria 3168, Australia
***Cancer Research Program, The Kinghorn Cancer Centre, Garvan Institute of Medical Research, 370 Victoria Street, Darlinghurst, Sydney, NSW 2010, Australia
†††Genentech, 1 DNA Way, MS 93, South San Francisco, CA 94010, U.S.A.

Protein kinase-like domains that lack conserved residues known to catalyse phosphoryl transfer, termed pseudokinases, have emerged as important signalling domains across all kingdoms of life. Although predicted to function principally as catalysis-independent protein-interaction modules, several pseudokinase domains have been attributed unexpected catalytic functions, often amid controversy. We established a thermal-shift assay as a benchmark technique to define the nucleotide-binding properties of kinase-like domains. Unlike *in vitro* kinase assays, this assay is insensitive to the presence of minor quantities of contaminating kinases that may otherwise lead to incorrect attribution of catalytic functions to pseudokinases. We demonstrated the utility of this method by classifying 31 diverse pseudokinase domains into four groups: devoid of detectable nucleotide or cation binding; cation-independent nucleotide binding; cation binding; and nucleotide binding enhanced by cations. Whereas nine pseudokinases bound ATP in a divalent cation-dependent manner, over half of those examined did not detectably bind nucleotides, illustrating that pseudokinase domains predominantly function as non-catalytic protein-interaction modules within signalling networks and that only a small subset is potentially catalytically active. We propose that henceforth the thermal-shift assay be adopted as the standard technique for establishing the nucleotide-binding and catalytic potential of kinase-like domains.

Key words: nucleotide binding, non-catalytic protein-interaction domain, protein kinase, pseudoenzyme, pseudokinase.

INTRODUCTION

Although first described in sea urchins [1], examples of pseudokinase domains are now known across all kingdoms of life. In previous years, essential functions in signal transduction have been attributed to these protein kinase-like domains, principally as modulators of the catalytic activities of *bona fide* protein kinases or as scaffolding proteins that nucleate the assembly of signalling complexes [2–14]. Often amid controversy, several pseudokinase domains have been reported to exhibit a low catalytic activity, yet the importance of this enzymatic activity to the protein's biological function and the ubiquity of this phenomenon across all pseudokinases remain unclear.

Pseudokinase domains were originally predicted to be devoid of any catalytic activity owing to the absence of one or more of the three crucial residues known to catalyse phosphoryl transfer

Abbreviations: AMP-PNP, adenosine 5′-[β,γ-imido]triphosphate; BPK1, bradyzoite pseudokinase 1; CASK, calcium/calmodulin-dependent serine protein kinase; CCK4, colon carcinoma kinase 4; CH2, calponin homology 2; CRN, CORYNE; DAP, *N*′2′-(4-aminomethyl-phenyl)-5-fluoro-*N*′4′-phenyl-pyrimidine-2,4-diamine; EphB6, Ephrin type-B receptor 6; ErbB3, v-erb-b2 avian erythroblastic leukaemia viral oncogene homologue 3; HER3, human epidermal growth factor receptor 3; ILK, integrin-linked kinase; IRAK, interleukin-1-receptor-associated kinase; ITC, isothermal titration calorimetry; JAK, Janus kinase; JH, JAK homology; KSR2, kinase suppressor of Ras 2; MLKL, mixed lineage kinase domain-like; NRBP1, nuclear receptor-binding protein 1; PEAK1, pseudopodium-enriched atypical kinase 1; PTK7, protein tyrosine kinase 7; ROP, rhoptry protein kinase; Ror1, receptor tyrosine kinase-like orphan receptor; RT-PCR, real-time PCR; RYK, receptor-like tyrosine kinase; SgK, sugen kinase; STRADα, STE20-related kinase adaptor α; TARK1, tomato atypical receptor-like kinase 1; TRB2, tribbles pseudokinase 2; TYK2, tyrosine kinase 2; ULK4, unc-51 like kinase 4; VRK3, vaccinia-related kinase 3.

[1] These authors contributed equally to this work.

[2] Correspondence may be addressed to either of these authors (email jamesm@wehi.edu.au or isabelle.lucet@monash.edu).

[3] Present address: Department of Pharmacology, University of Texas, Southwestern Medical Center, 6001 Forest Park Road, Dallas, TX 75390-9041, U.S.A.

[4] Present address: Department of Biological Sciences, Virginia Tech, 220 Ag Quad Lane, Blacksburg, VA 24061, U.S.A.

[5] Present address: Department of Biochemistry and Molecular Biology, School of Biomedical Sciences, Monash University, Clayton, Victoria 3800, Australia.

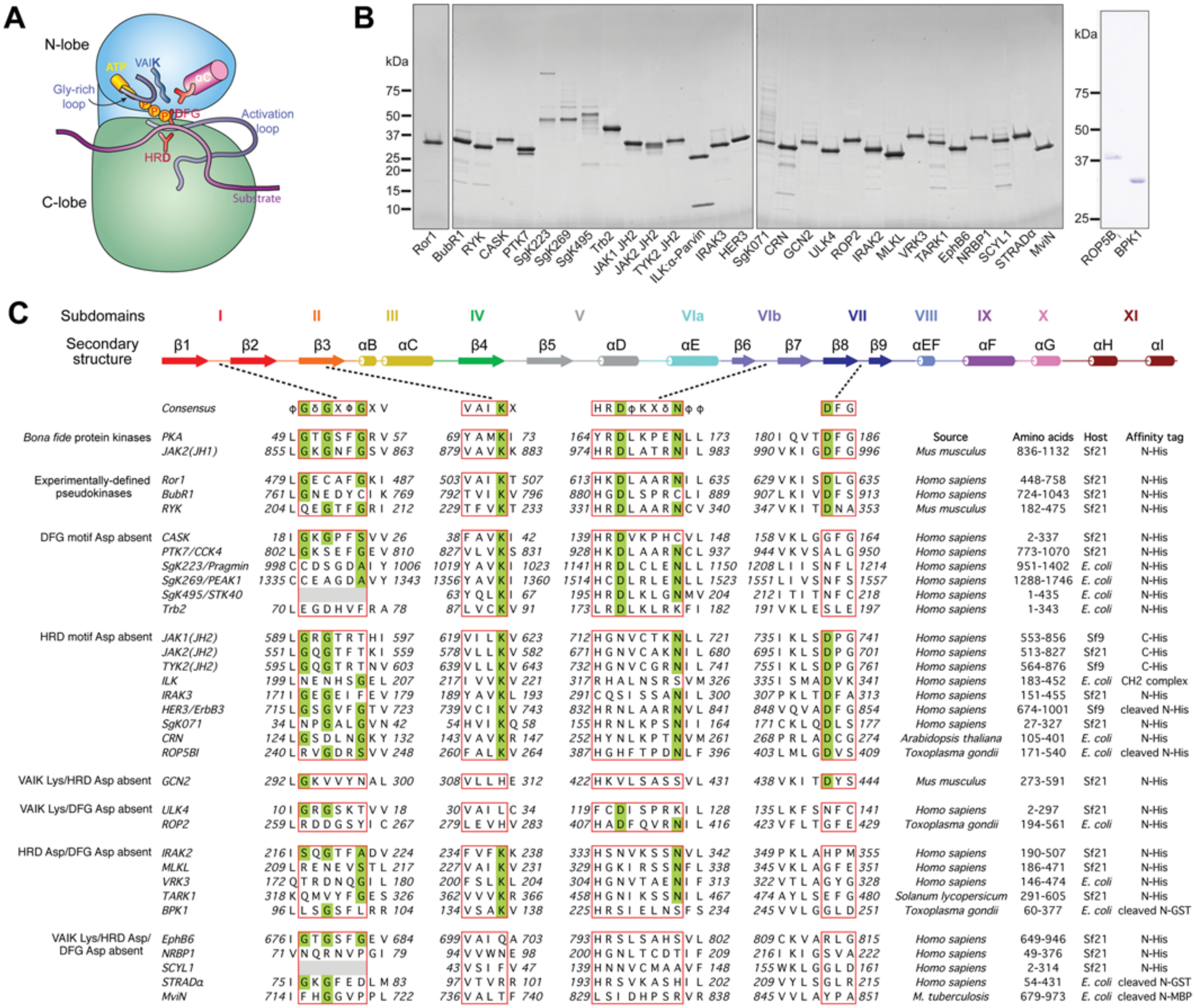

Figure 1 Pseudokinase domains selected for characterization of nucleotide binding

(**A**) Schematic cartoon of the eukaryotic protein kinase domain illustrating the amino acid motifs thought to be required for phosphoryl transfer that are usually absent from pseudokinase domains (depicted in the same style as [71]). (**B**) Purified pseudokinase domains (~1 μg) were resolved by reducing SDS/PAGE and then were Coomassie Blue-stained. Molecular mass markers are indicated on the left-hand side. In each case, the predominant species present in the preparation is the pseudokinase domain. (**C**) Multiple sequence alignment of canonical catalytic motifs in PKA (protein kinase A), a model serine/threonine protein kinase, and JAK2(JH1), a model tyrosine kinase, with the 31 pseudokinase domains examined in the present study. Consensus sequences of the catalytic motifs and the protein kinase secondary structure are depicted as described previously ([72] and [73]). φ, hydrophobic; δ, hydrophilic; Φ, large hydrophobic; X, any amino acid. Subdomains are labelled according to the nomenclature proposed in [15]. The G-loop and the VAIK, HRD and DFG motifs of catalytically active protein kinases and their pseudokinase counterparts are boxed in red, and residues thought to be essential for robust catalytic activity are shaded in green. Details of the species of origin, domain boundaries and expression strategy are given for each protein studied, with further details presented in the Experimental section and Supplementary Table S1 (at http://www.biochemj.org/bj/457/bj4570323add.htm). It should be noted that equivalent results were obtained for BubR1 with the domain boundaries of residues 720–1043 (results not shown).

in active protein kinases (Figure 1A). These residues are located within highly conserved motifs: (i) the VAIK motif, where the lysine residue in the β3 strand of the N-lobe positions the ATP α- and β-phosphates for catalysis; (ii) the HRD motif in the catalytic loop, which crucially contributes the catalytic aspartic acid residue; and (iii) the DFG motif within the activation loop contributes an aspartic acid residue involved in binding Mg^{2+} that stabilizes the bound ATP [15,16]. More recently, further consideration has been given to the integrity of the [GSA]xGxx[GSA] motif (where x is any amino acid) in the glycine-rich loop ('G-loop' or 'P-loop') that connects the β1 and β2 strands of the kinase domain N-lobe, since the flexibility of this loop is a key factor in promoting ATP binding [17]. Despite the absence of one or more of the three canonical catalytic residues, previous studies have reported nucleotide binding and enzymatic activities for a number of pseudokinases [14,18–21], raising the prospect that it might be a more general phenomenon of pseudokinases.

A prerequisite underlying whether a pseudokinase might exhibit catalytic activity is to define whether it binds to nucleotides in the presence of divalent cations. Having extensively reviewed the methods available to characterize the nucleotide-binding properties of pseudokinases [22], we used the most robust

technique, the thermal-shift assay, to examine nucleotide and divalent cation binding by pseudokinase domains *in vitro*. This assay obviates the need for specific fluorescently tagged nucleotides, such as TNP-ATP [2(3)-*O*-(2,4,6-trinitrophenyl) adenosine 5-triphosphate], which have been reported to bind targets with affinities several hundred-fold greater than ATP in some cases [23] or non-specifically fluoresce in the presence of BSA (P.A. Eyers and D. Ungureanu, unpublished work). Additionally, the assay monitors the thermal denaturation of the major protein species, so any minor contaminants, including co-purified protein kinases, that would lead to misleading results in radiometric *in vitro* kinase assays do not contribute to the signal. Using this assay, we experimentally defined the nucleotide- and divalent cation-binding properties of a collection of 31 diverse pseudokinase domains, including almost half of the human pseudokinome, and found that the majority of examined pseudokinases did not detectably bind nucleotides. The findings of the present study are consistent with the idea that these domains predominantly serve non-enzymatic functions in cellular signalling networks.

EXPERIMENTAL

Recombinant protein expression and purification

The sources of cDNA templates used in the preparation of the expression constructs are shown in Supplementary Table S1 (at http://www.biochemj.org/bj/457/bj4570323add.htm). Insect cell expression was performed using Sf21 cells [except for JAK1(JH2) (where JAK is Janus kinase and JH2 is JAK homology 1), TYK2(JH2) (where TYK2 is tyrosine kinase 2) and HER3 (human epidermal growth factor receptor 3)/ErbB3 (v-erb-b2 avian erythroblastic leukaemia viral oncogene homologue 3), which used Sf9 cells] as described previously [20] starting from the pFastBac HTb or pFastBac1 vectors (LifeTechnologies) or a pAceBac1-derived vector (ATG Biosynthetics) to generate His_6-tagged proteins. Bacterial expression constructs were prepared analogously to incorporate N-terminal His_6 tags. VRK3 (vaccinia-related kinase 3) and CRN (also known as CORYNE) were cloned into pProEX HTb (LifeTechnologies); SgK495 [sugen kinase 495; also known as STK40 (serine/threonine kinase 40)] and TRB2 [also known as TRIB2 (tribbles pseudokinase 2)] were cloned into pET30 Ek/LIC (Novagen); SgK223 and SgK269 [also known as PEAK1 (pseudopodium-enriched atypical kinase 1)] were cloned into pCOLD IV (Clontech); and ROP2 (rhoptry protein kinase 2) and BPK1 (bradyzoite pseudokinase 1) were cloned into pET28a (Clontech), and expression was performed according to established protocols [24]. Typically, proteins were purified using a standardized procedure [20], before Superdex-200 gel-filtration chromatography (GE Healthcare) in 200 mM NaCl, 20 mM Tris/HCl, 10 % (v/v) glycerol and 0.5 mM TCEP [tris-(2-carboxyethyl)phosphine] (pH 8.0).

The expression and purification of JAK2(JH1) [25,26], ILK (integrin-linked kinase)–α-parvin CH2 (calponin homology 2) domain complex [27], HER3/ErbB3 [4], MviN [28], $ROP5B_I$ [29], JAK2(JH2) [20] and STRADα (STE20-related kinase adaptor α) [30] were performed as described in their respective references. Typically, proteins were concentrated to 2 mg/ml or higher, snap-frozen in liquid N_2 and stored at $-80\,^{\circ}C$ until required. Protein concentrations were estimated on the basis of absorbance at 280 nm and the calculated molar absorption coefficients.

Thermal-shift assay for nucleotide binding

Thermal-shift assays were performed using a Corbett Real Time PCR machine with proteins diluted in 150 mM NaCl, 20 mM Tris/HCl (pH 8.0) and 1 mM DTT to 2–5 μM and assayed with the appropriate concentration of ligand in a total reaction volume of 25 μl. SYPRO Orange (Molecular Probes) was used as a probe with fluorescence detected at 530 nm. The temperature was raised in 1 °C per min steps from 25 °C to 95 °C and fluorescence readings were taken at each interval. Nucleotide- or cation-binding experiments were assessed relative to a buffer control. Two generic inhibitors, DAP {*N*′2′-(4-aminomethyl-phenyl)-5-fluoro-*N*′4′-phenyl-pyrimidine-2,4-diamine [31]; supplied by SYNthesis Med Chem} and VI16832 [32], were assessed relative to a 2 % (v/v) DMSO control. With the exception of the titration experiments, nucleotide concentrations of 0.2 mM, divalent cation concentrations of 1 mM, and DAP or VI16832 concentrations of 40 μM were used in each experiment. For each well, sample fluorescence was plotted as a function of increasing temperature. The melting temperature (T_m) corresponding to the midpoint for the protein unfolding transition was calculated by fitting the sigmoidal melt curve to the Boltzmann equation using GraphPad Prism, with R^2 values of >0.99. Data points after the fluorescence intensity maximum were excluded from fitting. Changes in the unfolding transition temperature compared with the control curve (ΔT_m) were calculated for each ligand (nucleotides $\pm$ cations). A positive ΔT_m value indicates that the ligand stabilizes the protein from denaturation, and therefore binds the protein. A minimum of two independent assays was performed for each protein and representative data are shown for each.

ITC

ITC (isothermal titration calorimetry) was performed using a MicroCal instrument (GE Healthcare). ATP (0.5 mM with no added divalent cations) was titrated into a solution of 50 μM human MLKL (mixed lineage kinase domain-like) pseudokinase domain at 25 °C. Both samples were prepared in 200 mM NaCl, 20 mM Hepes and 5 % (v/v) glycerol (pH 7.5).

RESULTS

Selection and preparation of target pseudokinase domains

A diverse group of pseudokinase domains were selected for expression, purification and nucleotide-binding studies to represent a cross-section of domains lacking different combinations of catalytic residues from the VAIK, HRD and DFG motifs (Figure 1). We also examined the proteins Ror1 (receptor tyrosine kinase-like orphan receptor 1), BubR1 [also known as BUB1B (BUB1 mitotic checkpoint serine/threonine kinase B)] and RYK (receptor-like tyrosine kinase), which despite containing the key residues of the VAIK, HRD and DFG motifs did not exhibit catalytic activity in earlier studies [33–36]. In addition to the 23 human and two mouse pseudokinases chosen for examination, we also analysed the bacterial pseudokinase MviN [28], two plant pseudokinases, CRN (CORYNE) [37] and TARK1 (tomato atypical receptor-like kinase 1) [38], and three *Toxoplasma gondii* pseudokinases, $ROP5B_I$ [29], ROP2 [39] and BPK1 [40].

In most cases, pseudokinases were overexpressed and purified from insect cells (Figures 1B and 1C). All were prepared either with a His_6 tag or proteolytically cleaved to remove globular affinity tags, such as GST and MBP (maltose-binding protein), since these domains will themselves undergo denaturation in the thermal-shift assay and may obscure detection of ligand binding to pseudokinase domains. Because some pseudokinase domains are unstable in their apo forms, we sought to test whether the assay was amenable to examining ligand binding

within protein complexes by examining ILK co-expressed and purified in complex with the CH2 domain of α-parvin [27,41]. Coomassie Blue-stained SDS/PAGE gels of the recombinant proteins examined in the present study are shown in Figure 1(B).

A thermal-shift assay for examining nucleotide and cation binding

Initially, we established an assay to evaluate nucleotide and cation binding to pseudokinase domains. The assay, based on an earlier method [42], monitors the thermal denaturation of a test protein by measuring the fluorescence arising from binding of the dye SYPRO Orange to hydrophobic patches that become exposed during denaturation. Ligand binding to a protein is known to enhance a protein's thermal stability, which manifests in an elevated melting temperature (T_m) that can be used to measure ligand binding. Relative to many other methods that have previously been explored to characterize nucleotide binding to kinase-like domains [22], the thermal-shift assay offers the following advantages: (i) modest quantities of recombinant protein (2–5 μg per condition) can be used; (ii) an RT-PCR (real-time PCR) instrument, a common piece of laboratory equipment, can be used; (iii) depending upon the RT-PCR instrument, 96 or 384 conditions can be tested simultaneously; (iv) the binding of any ligand, even a simple divalent cation such as Mg^{2+}, can be assessed without fluorescent tagging of the ligand; (v) the assay is extremely sensitive, being able to detect interactions with affinities in the 10^{-4} M range; and (vi) the presence of minor quantities of contaminating kinases will not affect the assay, since the denaturation measurement is dominated by the major species.

We validated our assay using human MLKL, whose mouse orthologue had already shown ATP binding in this assay [43]. We measured ATP binding to human MLKL by both thermal-shift assay and ITC, which yielded comparable K_d values ($\sim$15 μM; Supplementary Figures S1A and S1B at http://www.biochemj.org/bj/457/bj4570323add.htm). These studies, coupled with those reported previously for other kinases [44], provide important validation that the magnitudes of the thermal shifts correlate with ligand-binding affinities and thus that the thermal-shift assay provides an accurate representation of ligand binding. To gauge the sensitivity of the assay, we examined whether the assay could detect ADP–Mg^{2+} binding to the active tyrosine kinase domain of JAK2 (the 'JH1' domain), a domain we have previously shown to bind ADP–Mg^{2+} with a K_d value of $\sim$100 μM [45]. As shown in Supplementary Figures S1(C) and S1(D), we could indeed detect binding of JAK2(JH1) to a variety of nucleotides in the presence of Mg^{2+}, including ADP. On the basis of these preliminary studies, we estimated that this assay can detect ligand binding down to sub-millimolar K_d values. Indeed, a recent study using an alternative technique demonstrated that EphB6 (Ephrin type-B receptor 6) binds GTP–Mg^{2+} with a K_d value of $>$500 μM [46], and this interaction was also successfully detected in our assay (Figure 3C).

Classification of pseudokinases

We proceeded to qualitatively assess the propensity of each of 31 recombinant pseudokinase domains (Figure 1) to bind divalent cations (Mg^{2+} or Mn^{2+}), nucleotides {AMP, ADP, ATP, AMP-PNP (adenosine 5′-[β,γ-imido]triphosphate) and GTP} or both cation and nucleotide together. We also examined binding to two promiscuous ATP-competitive inhibitors, DAP [31] and VI16832 [32] (structures shown in Supplementary Figures S1E and S1F), as a means of evaluating whether the proteins contained an accessible, potentially druggable, pocket equivalent to the nucleotide-binding site of a catalytically active kinase. On the basis of our experience using this technique to screen for small molecule kinase inhibitors, we deemed a ΔT_m value of $\geqslant$3 °C to be a robust indicator of ligand binding.

On the basis of their ligand-binding properties in the thermal-shift assay, we categorized the 31 pseudokinases into four classes: (i) devoid of detectable nucleotide or cation binding; (ii) nucleotide binding; (iii) cation binding; and (iv) nucleotide and cation binding. As summarized in Table 1, more than half (16) of the pseudokinases did not detectably bind nucleotides or cations in our assay (Figure 2 and Supplementary Figure S2 at http://www.biochemj.org/bj/457/bj4570323add.htm). Interestingly, although we did not detect nucleotide or cation binding for TYK2(JH2) and IRAK3 (interleukin-1-receptor-associated kinase 3) (Figures 2E and 2F), both proteins were capable of binding the inhibitors DAP and VI16832, indicating the presence of an intact ATP-binding cleft and raising the possibility that these domains may bind nucleotides at affinities below the sensitivity of the assay. As shown in Figure 3, four proteins bound nucleotide alone [MLKL, EphB6, STRADα and ULK4 (unc-51 like kinase 4); Class 2] and two bound cations alone (SgK269 and ROP2; Class 3). It should be noted that the thermal shifts observed for Class 3 pseudokinases in the presence of nucleotides and cations can be accounted for by the presence of Mn^{2+} alone (Figures 3F and 3G). Fewer than one-third of the pseudokinase domains tested (9 of 31) bound nucleotide and cation: JAK1(JH2), JAK2(JH2), ILK, HER3/ErbB3, SgK071, CRN, ROP5B_1, IRAK2 and TARK1 (Figure 4 and Supplementary Figure S3 at http://www.biochemj.org/bj/457/bj4570323add.htm). Of note, our assay was amenable to examining the nucleotide and cation binding of pseudokinases within complexes with other protein-interaction domains. We were able to assay ILK (Figure 4C and Supplementary Figure S3C), even though its stability relies on being in complex with the α-Parvin CH2 domain.

RYK contains each of the three canonical residues present in active protein kinases, but is known to be catalytically inactive [36] and did not detectably bind nucleotides or cations in our assays. To test whether the highly conserved phenylalanine residue within the TFVK sequence, the counterpart of a conventional kinase's VAIK motif, might occupy the adenine-binding pocket and prevent nucleotide binding, we examined a TFVK>VAVK mutant RYK by thermal shift. Although this mutation did not result in detectable nucleotide binding, the mutant was able to engage the promiscuous ATP-competitive inhibitor DAP, whereas wild-type RYK did not (Figures 2B and 2C). ATP binding by a second protein, EphB6, was not enhanced by the presence of divalent cations (Figure 3C), leading us to query whether the R^{813}LG sequence in place of the canonical DFG motif might serve a role in binding the γ-phosphate of ATP, effectively supplanting the conventional Mg^{2+}. Introduction of the R813D mutation abrogated the direct binding of ATP by EphB6 in the absence of cations, but conferred an unexpected ability to bind ATP in the presence of Mn^{2+} (Figure 3D).

It is surprising that BubR1, which contains the catalytic residues typical of an active protein kinase, did not bind nucleotides in the presence or absence of divalent cations (Figure 2A). To ensure that this was not a consequence of the domain boundaries (residues 724–1043) we used initially, we also characterized a longer construct (residues 720–1043), similar to that used in [35], which contains the kinase extension domain that is critical for catalytic activity of the related *bona fide* protein kinase BUB1 [47]. We expressed BubR1 in both Sf21 and *Escherichia coli* cells and found that all preparations behaved equivalently in the thermal-shift assay (results not shown), confirming the inability of BubR1 to detectably bind to nucleotides or divalent cations.

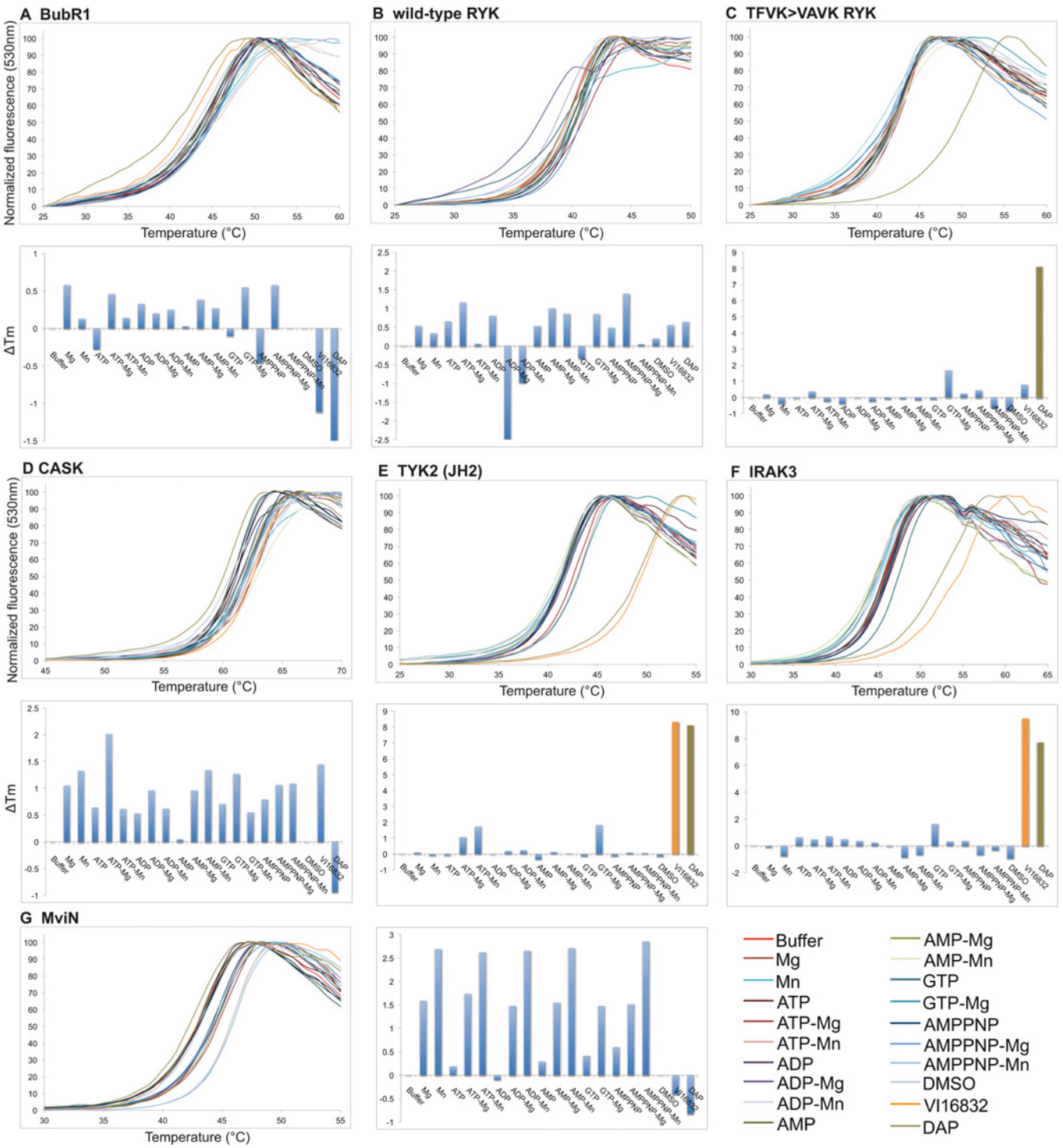

Figure 2 Thermal denaturation curves for selected Class 1 (non-binding) pseudokinase domains

Thermal denaturation curves of the Class 1 pseudokinases, BubR1 (**A**), wild-type RYK (**B**), CASK (**D**) and MviN (**G**) (upper panels) with the corresponding histograms depicting the ΔT_m values in each condition (lower panels), as derived from analysis of upper panel curves. Although thermal denaturation of TFVK>VAVK RYK (**C**) and IRAK3 (**F**) was not affected by nucleotides or cations, TYK2(JH2) (**E**) exhibited modest, but consistent, thermal shifts between experiments in the presence of ATP–Mg^{2+}, ATP–Mn^{2+} or GTP–Mg^{2+}. Thermal shifts for all three of these proteins were detected in the presence of the inhibitor VI16832 and/or DAP. A colour key for the curve labelling is to the right-hand side of the curves. In the histograms, bars are coloured according to the colour key when $\Delta T_m > 3$ °C and pale blue otherwise. Thermal denaturation curves for the other Class 1 pseudokinases, Ror1, PTK7/CCK4, SgK223, SgK495, TRB2, GCN2 [also known as EIF2AK4 (eukaryotic translation initiation factor 2-α kinase 4)], VRK3, BPK1, NRBP1 and SCYL1 (SCY1-like 1), are shown in Supplementary Figure S2 (at http://www.biochemj.org/bj/457/bj4570323add.htm).

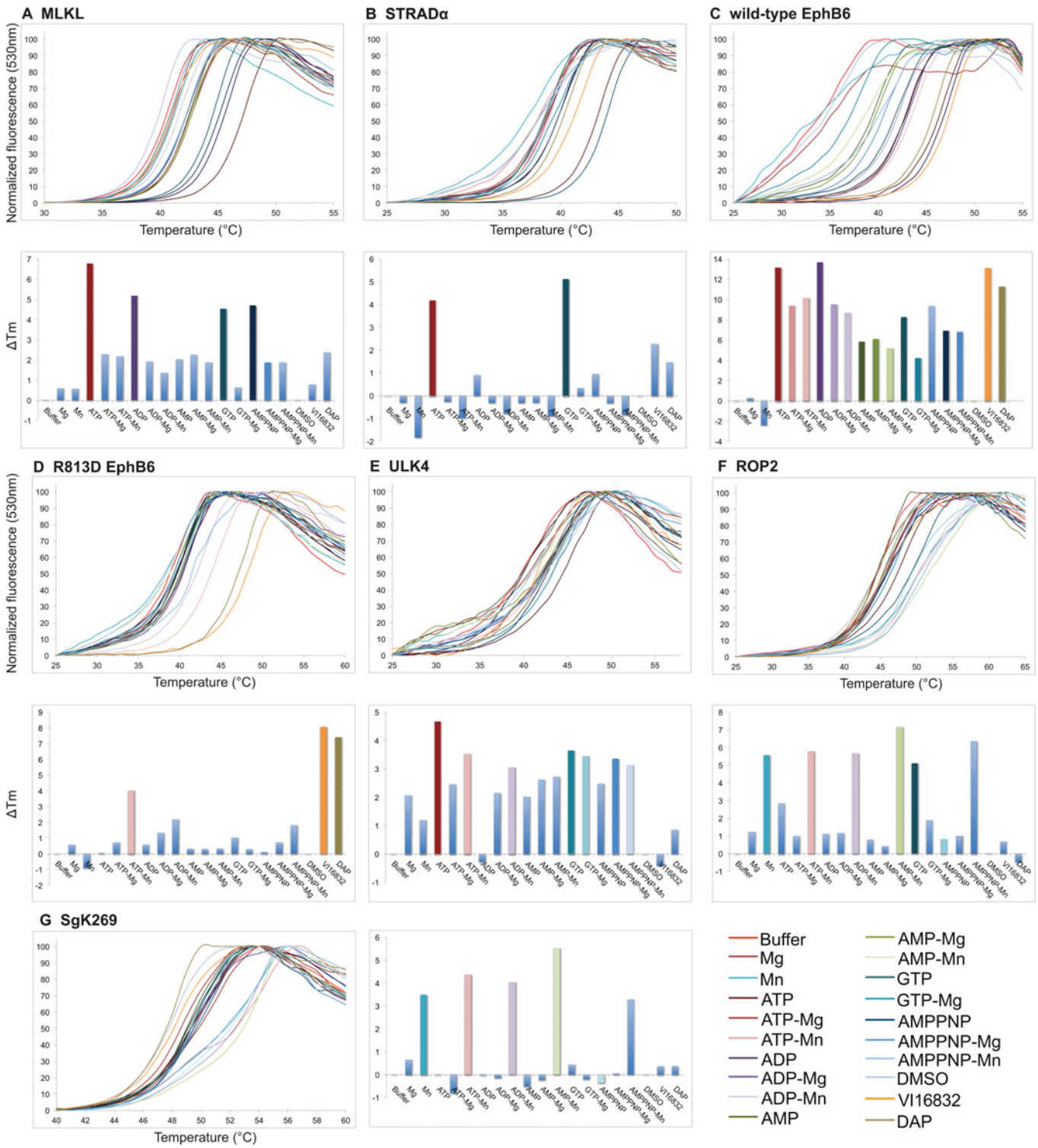

Figure 3 Thermal denaturation curves and ΔT_m analyses of Class 2 (nucleotide binding) and Class 3 (cation binding) pseudokinases

Thermal denaturation data of the Class 2 pseudokinases, MLKL (**A**), STRADα (**B**), wild-type EphB6 (**C**) and ULK4 (**E**), presented as described in the legend to Figure 2. (**D**) The R813D mutation converts EphB6 from a Class 2 into Class 4 pseudokinase. Note that wild-type EphB6 (**C**) and ULK4 (**E**) are classified as Class 2 (nucleotide-binding) as the presence of Mn^{2+} and Mg^{2+} does not enhance ATP binding. Data for the Class 3 (cation-binding) pseudokinases ROP2 and SgK269 are presented in (**F**) and (**G**) respectively. Note that ROP2 and SgK269 are classified as Class 3 (cation-binding) pseudokinases because the presence of nucleotides does not confer further thermal stability above and beyond that of cation alone.

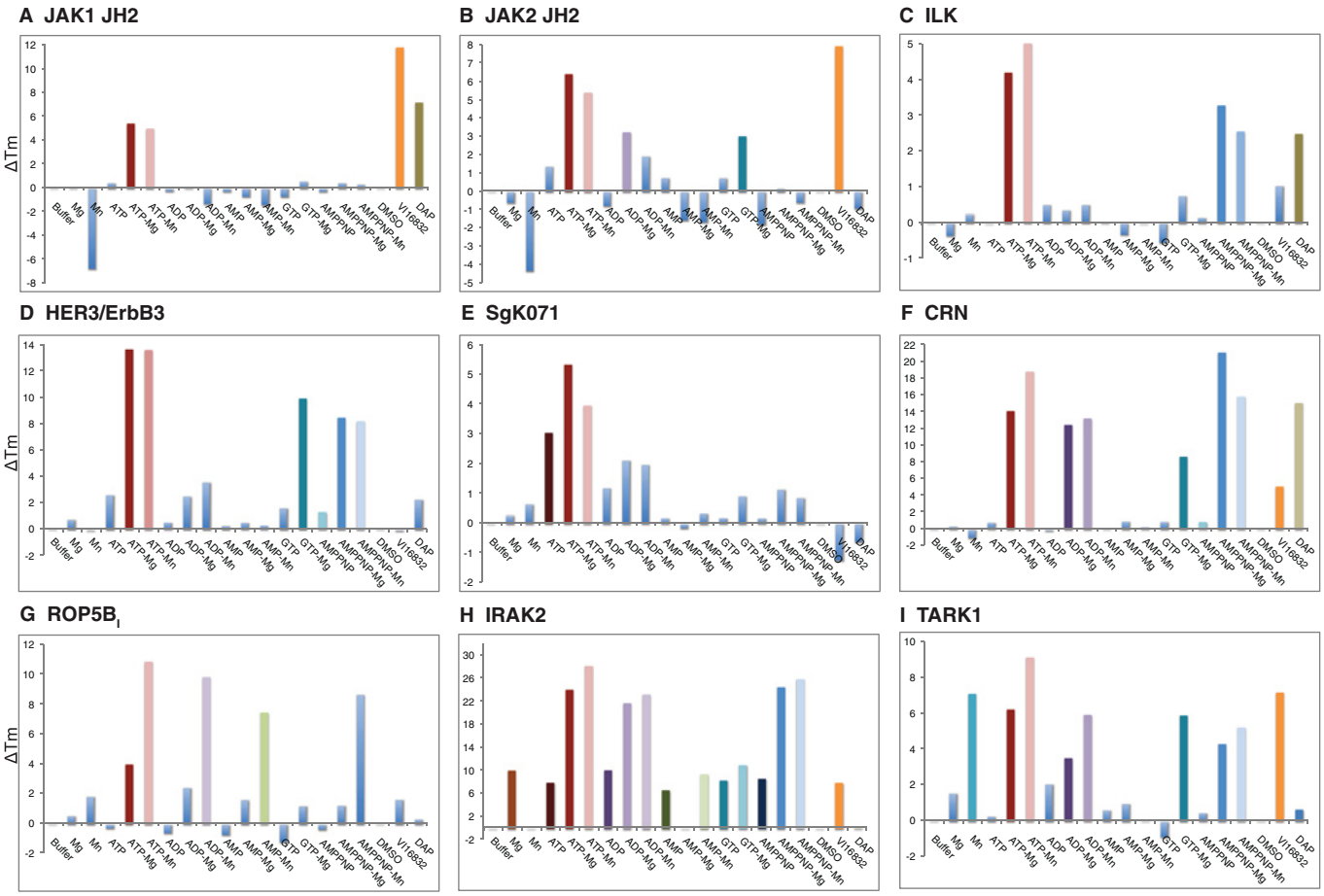

Figure 4 ΔT_m analyses of Class 4 (nucleotide- and cation-binding) pseudokinases

Histograms depicting the ΔT_m value in each condition derived from thermal denaturation curves presented in Supplementary Figure S3 (at http://www.biochemj.org/bj/457/bj4570323add.htm) for JAK1(JH2) (**A**), JAK2(JH2) (**B**), ILK (**C**), HER3/ErbB3 (**D**), SgK071 (**E**), CRN (**F**), ROP5B$_I$ (**G**), IRAK2 (**H**) and TARK1 (**I**). Note that some conditions are destabilizing, leading to negative ΔT_m values. TARK1 (**I**) was categorized as Class 4 owing to the observation of ATP–Mg^{2+}, ADP–Mg^{2+}, AMP-PNP–Mg^{2+} and GTP–Mg^{2+} binding. Interestingly TARK1 also appears to bind Mn^{2+} in the absence of nucleotides, leading to thermal-stability shifts under all Mn^{2+}-containing conditions.

DISCUSSION

The importance of pseudokinases to cellular signalling has only recently begun to be appreciated. Fuelled by the discovery that mutations within the pseudokinase domain of JAK2 underlie human blood cell malignancies [48–52], pseudokinases have emerged as an unexplored family of therapeutic targets. Previous studies have attributed unexpected catalytic functions to several pseudokinase domains, including that of JAK2 [20], ErbB3 [19] and KSR2 (kinase suppressor of Ras 2) [14], although whether nucleotide-binding and, relatedly, phosphoryl transfer activity is a widespread property within this domain family has remained unclear. We have addressed this issue by profiling the nucleotide-binding properties of a collection of 31 diverse pseudokinase domains using a robust thermal-shift assay.

Thermal-shift assay data are supported by prior structural studies

Although we have performed a comprehensive examination of ATP, ADP, AMP, AMP-PNP and GTP binding in the presence or absence of Mg^{2+} or Mn^{2+} in the present study, structural and biophysical studies have previously explored the ATP-binding capacities of some pseudokinases included in the present study [4,17–19,22,27–30,39,41,53,54]. With the exception of CASK (calcium/calmodulin-dependent serine protein kinase), all of these prior findings are supported by the present study, providing a sound foundation for the results reported in the present paper for formerly uncharacterized pseudokinases. The absence of ATP binding to CASK using the thermal-shift assay is unsurprising (Figure 2D), since our interpretation of the prior CASK ATP-binding data [18] suggests a K_d(ATP) value in the millimolar range, an affinity beyond the range of detection using most biophysical techniques. Accordingly, we were unable to detect nucleotide binding to CASK prepared from *E. coli* (results not shown) or insect cells (Figure 2D). The structure of the TYK2(JH2) domain bound to an ATP-mimetic inhibitor was recently solved (PDB code 3ZON), confirming the presence of an accessible active site: a finding consistent with the binding to the small-molecule kinase inhibitors DAP and VI16832 observed in the present study (Figure 2E). Although the structure of the Ror1 pseudokinase domain has not yet been solved, an absence of ATP binding in the present study can be rationalized by inspection of the structures of the related Ror2 (PDB codes 3ZZW and 4GT4)

Table 1 Summary of nucleotide, divalent cation and inhibitor binding by pseudokinases

The G-loop was defined as degraded if two of three positions do not conform to the sequence [GSA]xGxx[GSA] where x is any amino acid.

(a) Class 1 (devoid of nucleotide- or cation-binding)

Pseudokinase	Degraded G-loop	VAIK motif lysine residue present	HRD motif aspartic acid residue present	DFG motif aspartic acid residue present	DAP or VI16832 binding
Ror1	No	+	+	+	−
BubR1	Yes	+	+	+	−
RYK	No	+ (TFVK)*	+	+ (DNA)*	−
RYK TFVK>VAVK	No	+	+	+ (DNA)*	+ (DAP)
CASK	No	+	+	−	−
PTK7/CCK4	No	+	+	−	−
SgK223	Yes	+	+	−	−
SgK495/STK40	Yes	+	+	−	−
TRB2	Yes	+	+	−	−
TYK2(JH2)	No	+	−	+	+
IRAK3	No	+	−	+	+
GCN2	Yes	−	−	+	−
VRK3	Yes	+	−	−	−
BPK1	Yes	+	−	−	−
NRBP1	Yes	−	−	−	−
SCYL1	Yes	−	−	−	−
MviN	Yes	−	−	−	−

(b) Class 2 (nucleotide-binding)

Pseudokinase	Degraded G-loop	VAIK motif lysine residue present	HRD motif aspartic acid residue present	DFG motif aspartic acid residue present	DAP or VI16832 binding
ULK4	No	−	+ (FCD)*	−	−
MLKL	Yes	+	−	−	−
EphB6	No	−	−	−	+
STRADα	No	− (VTVR)*	−	−	−

(c) Class 3 (cation-binding)

Pseudokinase	Degraded G-loop	VAIK motif lysine residue present	HRD motif aspartic acid residue present	DFG motif aspartic acid residue present	DAP or VI16832 binding
SgK269	Yes	+	+	−	−
ROP2	Yes	−	+	−	−

(d) Class 4 (nucleotide- and cation-binding)

Pseudokinase	Degraded G-loop	VAIK motif lysine residue present	HRD motif aspartic acid residue present	DFG motif aspartic acid residue present	DAP or VI16832 binding	Catalytic activity?
JAK1(JH2)	No	+	−	+	+	No [70]
JAK2(JH2)	No	+	−	+	+ (VI16832)	Yes [20,53]
ILK	Yes	+	−	+ (DVK)*	−	No [27,41]
HER3/ErbB3	No	+	−	+	−	Yes [19]
SgK071	No	+	−	+	−	Unknown
CRN	No	+	−	+	+	No [37]
ROP5B$_I$	No	+	−	+	−	No [29]
IRAK2	No	+	−	−	+ (VI16832)	Unlikely [66,67]
TARK1	Yes	+	−	− (EFG)*	+ (VI16832)	No [38]
EphB6 R813D	No	−	−	+	+	Unknown

*Motif sequence noted due to similarity/difference from conventional motif

[55], where the adenine-binding pocket is partly occupied by the side chain of the highly conserved Tyr^{555}.

Pseudokinases function principally as catalysis-independent protein-interaction modules

The largest class of pseudokinases observed in the present study did not detectably bind nucleotides or divalent cations (Class 1; Figure 2 and Table 1, and Supplementary Figure S2), providing compelling support for the hypothesis that pseudokinase domains serve predominantly non-catalytic functions within signalling networks in Nature. Of these, Ror1 [33,34], RYK [36], CCK4 (colon carcinoma kinase 4)/PTK7 (protein tyrosine kinase 7) [56], BubR1 [35], IRAK3/IRAK-M [57] and MviN [28] were not catalytically active *in vitro* in previously published studies, consistent with our observations that they do not bind ATP.

Nucleotide-binding (Class 2) pseudokinases

Prior studies of the nucleotide-binding-only proteins STRADα and EphB6 did not reveal kinase activity *in vitro* [30,58,59], in keeping with our premise that both ATP and cation binding are

necessary for catalytic activity. Human MLKL has previously been attributed a catalytic function based on *in vitro* kinase assays with protein immunoprecipitated from HEK (human embryonic kidney)-293T cells [60]. However, on the basis of our previous characterization of mouse MLKL [43], and the analogous cation-independent nucleotide-binding properties observed for human MLKL in the present study, it is probable that the catalytic activity previously attributed to MLKL is likely to arise from the catalytic activity of a contaminating protein. A fourth protein, ULK4, has not been characterized biochemically, though cation-independent nucleotide binding indicates that ULK4 will similarly serve non-catalytic signalling roles.

A common feature of STRADα, MLKL, EphB6 and ULK4 is divergent sequences in place of the conventional cation-binding DFG motif. In the case of STRADα and EphB6, the DFG motif is replaced by GLR and RLG respectively. Since the GLR sequence was shown to play a key role in mediating ATP binding by STRADα [30], we examined whether the R^{813}LG counterpart in EphB6 might play a similar role. R813D mutant EphB6 exhibited a predictable loss of nucleotide binding in the absence of divalent cations in the thermal-shift assay, but an unexpected gain of Mn^{2+}-dependent ATP binding (Figure 3D). This finding is intriguing, since the RLG>DLG mutation confers nucleotide-binding properties on EphB6 that are synonymous with a conventional protein kinase, although in the absence of a catalytic residue in the catalytic loop, we anticipate that R813D EphB6 will not be enzymatically active. An examination of orthologous sequences revealed that the arginine residue of the RLG motif is conserved almost universally as one of two basic residues (arginine or histidine) in mammalian EphB6 orthologues, whereas other orthologues, including those in fish (including lamprey), chicken, zebra finch and turkey, contain a DFG sequence in addition to intact VAIK (or VAVK) and HRD motifs. These observations indicate that mammalian EphB6 orthologues evolved from a catalytically active ancestral protein kinase to serve non-catalytic nucleotide-binding functions in cell signalling, presumably as means of modulating protein conformation. Remarkably, the evolution of the RLG sequence in place of the canonical DFG motif has co-evolved with substitutions within the VAIK and HRD motifs. Our findings demonstrate an important role for the RLG sequence in facilitating nucleotide binding in mammalian EphB6 orthologues that is likely to have evolved to compensate for the concomitant substitution of the VAIK motif to VAIQ. The existence of the Class 2 pseudokinases provides important support for the emerging idea that nucleotide binding among pseudokinases may have evolved as a non-catalytic conformational switch, as proposed for STRADα [30,54] and MLKL [43]. An exciting possibility is that conformational regulation by nucleotide binding, rather than catalytic functions, may similarly underlie the functions of Class 4 pseudokinases as protein-interaction modules within signalling networks.

The Class 2 pseudokinases also offer important mechanistic insights into the contributions of the VAIK motif lysine residue to ATP binding in both pseudokinases and catalytically active kinases. Consistent with a prior study of the *bona fide* protein kinase Lck (lymphocyte-specific protein tyrosine kinase) [61], where the VAIK motif lysine residue was shown to serve a catalytic rather than ATP-binding function, we observed that ATP binding was still accomplished by EphB6 and ULK4 (Figures 3C and 3E), two pseudokinases containing VAIQ and VAIL respectively in place of the canonical VAIK motif. In some pseudokinase domains, however, it appears that the VAIK motif lysine residue has evolved an essential role in ATP binding, as illustrated by mutational analyses of mouse [43] and human [62] MLKL, both Class 2 pseudokinases, and HSER (heat-stable enterotoxin receptor)/GC-C (guanylate cyclase C) [63]. As a result, it appears that in the absence of other key ATP- and/or divalent cation-binding residues, some pseudokinases have evolved a greater reliance on the VAIK motif lysine residue to mediate ATP binding. Furthermore, these findings raise the intriguing possibility that the VAIK motif lysine residue may mediate ATP binding, rather than have a catalytic function, in a subset of catalytically active protein kinases.

Cation-binding (Class 3) pseudokinases

Pseudokinases that bound divalent cations alone include SgK269/PEAK1 and the *T. gondii* protein ROP2 (Figures 3F and 3G and Table 1). Consistent with the original study of ROP2 [39], we observed no ATP binding in our assays although, curiously, we did detect GTP binding in a cation-independent manner. This observation is most consistent with ROP2 containing an intact nucleotide-binding pocket that allows ROP2 to retain either a Mn^{2+}- or GTP-binding capacity, albeit in the absence of catalytic activity. By comparison, SgK269 had previously been attributed a catalytic activity [64,65], although in our hands it did not detectably bind ATP: a finding more consistent with the highly degraded G-loop and the absence of the conserved aspartic acid residue in the DFG motif. Interestingly, SgK223, a protein closely related to SgK269, likewise did not bind nucleotides in our assays, but, in contrast with SgK269, did not bind Mn^{2+} ions (Supplementary Figure S2B). It should be noted that the bacterial pseudokinase MviN showed evidence of Mn^{2+} binding, but because the ΔT_m value in the presence of Mn^{2+} was $<3\,^{\circ}C$, it did not meet our criteria to be categorized as cation binding (Figure 2G).

Nucleotide- and cation-binding (Class 4) pseudokinases

The prevalence of Class 1 pseudokinases and the identification of Classes 2 and 3 demonstrate that the catalytic activity attributed to a subset of pseudokinase domains is not a widespread feature. We deemed nine of the 31 pseudokinases examined in the present study to be potentially catalytically active on the basis of the premise that both nucleotide and cation must be bound simultaneously for efficient phosphoryl transfer. Of these Class 4 pseudokinases (Figure 4), catalytic activities have been reported for purified recombinant JAK2(JH2) [20] and ErbB3/HER3 [19], indicating that in some pseudokinases asparagine residues can substitute (albeit poorly) for the catalytic aspartic acid of the canonical HRD motif. IRAK2 immunoprecipitated from macrophages was previously attributed a catalytic function [66], although this has been recently queried [67]. In addition, on the basis of our JAK2(JH2) data, we anticipated that the related proteins, JAK1(JH2) and TYK2(JH2), would behave similarly to JAK2(JH2). Unexpectedly, we observed that TYK2(JH2) exhibited only modest, albeit consistent, thermal shifts in the presence of ATP–Mg^{2+}, ATP–Mn^{2+} or GTP–Mg^{2+} (Figure 2E), indicating that TYK2(JH2) may bind nucleotides in a cation-dependent manner, but with affinities below the sensitivity of our assay. In contrast, recent comprehensive structure/function studies have demonstrated that the pseudokinase domain of ILK is completely devoid of catalytic activity owing to a severely degraded catalytic core, and catalysis-independent functions have been elegantly established using knockin studies of ILK kinase-dead mutants in mice [68]. In addition, CRN, $ROP5B_1$ and TARK1 did not exhibit catalytic activity in published studies [29,37,38], supporting the idea that nucleotide binding by pseudokinase

domains predominantly serves a role in modulating protein conformation, rather than catalytic functions, in cell signalling.

Can nucleotide-binding properties be predicted from pseudokinase amino acid sequences?

Although the nucleotide- and cation-binding (Class 4) pseudokinases constitute less than one-third of those profiled in the present paper, these domains were considered the most likely to be catalytically active and, as a result, we discuss some trends among this group that might aid their prediction in the future. First, combined G-loop degradation and the loss of the VAIK, DFG and HRD motifs thwarts nucleotide and cation binding and, accordingly, such sequence divergence is predictive of a catalytically inactive pseudokinase domain. Secondly, the DFG motif aspartic acid residue is present in nearly all pseudokinases that bind VI16832, DAP or nucleotide and cation (Table 1). Finally, among pseudokinase domains that bind nucleotide and cation (Class 4), the VAIK motif lysine residue (or, in some cases, arginine, such as in KSR2 [14]) and the DFG motif aspartic acid [or, in some cases, glutamic acid, such as in TARK1 (the present study)] are almost entirely conserved, with loss of only the catalytic aspartic acid from the HRD motif evident throughout Class 4. The sole loss of the catalytic aspartic acid residue in the HRD motif is not deleterious to nucleotide binding, since this catalytic residue is typically peripheral to the bound nucleotide and divalent cation in conventional protein kinases. Although not essential for nucleotide and cation engagement, the loss of the catalytic aspartic acid residue from the HRD motifs in the Class 4 pseudokinases is likely to severely limit their capacity to catalyse the phosphoryl transfer reaction. However, as noted previously [69], it remains unclear at this point how much catalytic activity is required *in vivo* for pseudokinases to play a significant role in modulating signal transduction and, as discussed above, whether ATP binding might principally serve as a conformational switch that governs the capacities of pseudokinases to serve as protein-interaction domains.

Another trend that we observed is that, in general, Class 4 pseudokinases were less thermostable than Class 1. Although the T_m values of Class 1 pseudokinases were typically $>40\,^{\circ}C$, with $T_m>50\,^{\circ}C$ observed for PTK7, BPK1, NRBP1 (nuclear receptor-binding protein 1) and CASK, Class 4 proteins typically exhibited lower T_m values ($<40\,^{\circ}C$), suggesting a high degree of flexibility between the N- and C-lobes corresponding to a more 'open' ATP-binding cleft in the absence of ligand. Exceptions to this generalization, such as the high thermal stability of the Class 4 protein ROP5B$_I$ (Supplementary Figure S3G), prevent thermal stability itself serving diagnostically as an indicator of the nucleotide-binding propensity. Nonetheless these data raise the interesting possibility that, for Class 2 and 4 pseudokinases, the significant stabilization induced by ATP binding may be central to their ability to act as conformational switches or rigid scaffolds for intermolecular interactions.

Although a comprehensive understanding of this important family of domains awaits further biochemical, structural and biological characterization, the methodology and data of the present study provide a foundation for identifying pseudokinase domains that have retained a functional nucleotide-binding pocket. This subset of pseudokinase domains, including those known to be mutated in human cancers, such as JAK2(JH2) and HER3/ErbB3, are potentially druggable by ATP-competitive small molecules that could either inhibit weak catalytic activities or modulate the conformations of pseudokinases that serve as molecular switches in signalling pathways [30,43,54]. Consequently, these pseudokinases represent an exciting emergent class of drug targets. To this end, in future, we envisage that the methodology described in the present study will be utilized to screen for small-molecule lead compounds from which specific therapeutic modulators of pseudokinase functions could be developed.

AUTHOR CONTRIBUTION

The present study was designed and supervised by James Murphy and Isabelle Lucet. James Murphy, Qingwei Zhang, Samuel Young, Leila Varghese, Kelan Chen, Anne Tripaydonis, Jeffrey Babon and Isabelle Lucet performed the experiments. Michael Reese, Fiona Bailey, Patrick Eyers, Daniela Ungureanu, Henrik Hammaren, Olli Silvennoinen, Natalia Jura, Koichi Fukuda, Jun Qin, Zachary Nimchuk, Mary Beth Mudgett, Sabine Elowe, Christine Gee, Ling Liu and Roger Daly contributed vital reagents. James Murphy, Gerard Manning, Jeffrey Babon and Isabelle Lucet analysed the data with input from all of the other authors. James Murphy, Jeffrey Babon and Isabelle Lucet wrote the paper with input from all of the other authors.

ACKNOWLEDGEMENTS

We thank Professor Dario Alessi (University of Dundee, Dundee, U.K.) for providing the GST–STRADα expression construct; Professor Seung-Taek Lee (Yonsei University, Seoul, Korea) for the PTK7/CCK4 template DNA; Dr Alessandra Gentile (Institute for Cancer Research and Treatment, Candiolo, Italy) for the Ror1 template cDNA; Dr Elton Zeqiraj (Tanenbaum-Lunenfeld Research Institute, Toronto, Canada) for assistance with the secondary-structure cartoon in Figure 1(C); and the Monash University Protein Production Unit for access to the Corbett RT-PCR instrument used for all of the thermal-shift assays.

FUNDING

This work was supported by the National Health and Medical Research Council (NHMRC) [grant numbers 637342 and 1011804]; the Australian Research Council (ARC) [fellowships FT100100100 and FT110100169 (to J.M.M. and J.J.B.)]; the Leukaemia Foundation and the Australian Stem Cell Centre via scholarships to L.N.V.; the National Institutes of Health (NIH) [grant numbers R01 HL58758 (to J.Q.) and AI73756 (to M.L.R.)]; the Medical Research Council of Academy of Finland, the Sigrid Juselius Foundation, the Medical Research Fund of Tampere University Hospital, the Finnish Cancer Foundation and the Tampere Tuberculosis Foundation (to O.S.); the American Heart Association [grant number 11BGIA7440051 (to N.J.)]; and the National Science Foundation [grant number IOS-0821801 (to M.B.M.)]; with additional support from the Victorian State Government Operational Infrastructure Support and the NHMRC Independent Research Institutes Infrastructure Support Scheme (IRIISS) [grant number 361646].

REFERENCES

1 Singh, S., Lowe, D. G., Thorpe, D. S., Rodriguez, H., Kuang, W. J., Dangott, L. J., Chinkers, M., Goeddel, D. V. and Garbers, D. L. (1988) Membrane guanylate cyclase is a cell-surface receptor with homology to protein kinases. Nature **334**, 708–712

2 Baas, A. F., Boudeau, J., Sapkota, G. P., Smit, L., Medema, R., Morrice, N. A., Alessi, D. R. and Clevers, H. C. (2003) Activation of the tumour suppressor kinase LKB1 by the STE20-like pseudokinase STRAD. EMBO J. **22**, 3062–3072

3 Boudeau, J., Miranda-Saavedra, D., Barton, G. J. and Alessi, D. R. (2006) Emerging roles of pseudokinases. Trends Cell Biol. **16**, 443–452

4 Jura, N., Shan, Y., Cao, X., Shaw, D. E. and Kuriyan, J. (2009) Structural analysis of the catalytically inactive kinase domain of the human EGF receptor 3. Proc. Natl. Acad. Sci. U.S.A. **106**, 21608–21613

5 Keeshan, K., Bailis, W., Dedhia, P. H., Vega, M. E., Shestova, O., Xu, L., Toscano, K., Uljon, S. N., Blacklow, S. C. and Pear, W. S. (2010) Transformation by Tribbles homolog 2 (Trib2) requires both the Trib2 kinase domain and COP1 binding. Blood **116**, 4948–4957

6 Saharinen, P., Takaluoma, K. and Silvennoinen, O. (2000) Regulation of the Jak2 tyrosine kinase by its pseudokinase domain. Mol. Cell. Biol. **20**, 3387–3395

7 Yu, H., He, K., Li, L., Sun, L., Tang, F., Li, R., Ning, W. and Jin, Y. (2013) Deletion of Stk40 in the mouse causes respiratory failure and death at birth. J. Biol. Chem. **288**, 5342–5352

8 Burman, J. L., Bourbonniere, L., Philie, J., Stroh, T., Dejgaard, S. Y., Presley, J. F. and McPherson, P. S. (2008) Scyl1, mutated in a recessive form of spinocerebellar neurodegeneration, regulates COPI-mediated retrograde traffic. J. Biol. Chem. **283**, 22774–22786

9 Fleckenstein, M. C., Reese, M. L., Konen-Waisman, S., Boothroyd, J. C., Howard, J. C. and Steinfeldt, T. (2012) A *Toxoplasma gondii* pseudokinase inhibits host IRG resistance proteins. PLoS Biol. **10**, e1001358

10 Wilson, C. H., Crombie, C., van der Weyden, L., Poulogiannis, G., Rust, A. G., Pardo, M., Gracia, T., Yu, L., Choudhary, J., Poulin, G. B. et al. (2012) Nuclear receptor binding protein 1 regulates intestinal progenitor cell homeostasis and tumour formation. EMBO J. **31**, 2486–2497

11 Croucher, D. R., Hochgrafe, F., Zhang, L., Liu, L., Lyons, R. J., Rickwood, D., Tactacan, C. M., Browne, B. C., Ali, N., Chan, H. et al. (2013) A novel signaling pathway in basal breast cancer involving Lyn and the atypical kinase SgK269/PEAK1. Cancer Res. **73**, 1969–1980

12 Zheng, Y., Zhang, C., Croucher, D. R., Soliman, M. A., St-Denis, N., Pasculescu, A., Taylor, L., Tate, S. A., Hardy, W. R., Colwill, K. et al. (2013) Temporal regulation of EGF signalling networks by the scaffold protein Shc1. Nature **499**, 166–171

13 Eyers, P. A. and Murphy, J. M. (2013) Dawn of the dead: protein pseudokinases signal new adventures in cell biology. Biochem. Soc. Trans. **41**, 969–974

14 Brennan, D. F., Dar, A. C., Hertz, N. T., Chao, W. C., Burlingame, A. L., Shokat, K. M. and Barford, D. (2011) A Raf-induced allosteric transition of KSR stimulates phosphorylation of MEK. Nature **472**, 366–369

15 Hanks, S. K., Quinn, A. M. and Hunter, T. (1988) The protein kinase family: conserved features and deduced phylogeny of the catalytic domains. Science **241**, 42–52

16 Manning, G., Whyte, D. B., Martinez, R., Hunter, T. and Sudarsanam, S. (2002) The protein kinase complement of the human genome. Science **298**, 1912–1934

17 Scheeff, E. D., Eswaran, J., Bunkoczi, G., Knapp, S. and Manning, G. (2009) Structure of the pseudokinase VRK3 reveals a degraded catalytic site, a highly conserved kinase fold, and a putative regulatory binding site. Structure **17**, 128–138

18 Mukherjee, K., Sharma, M., Urlaub, H., Bourenkov, G. P., Jahn, R., Sudhof, T. C. and Wahl, M. C. (2008) CASK functions as a Mg^{2+}-independent neurexin kinase. Cell **133**, 328–339

19 Shi, F., Telesco, S. E., Liu, Y., Radhakrishnan, R. and Lemmon, M. A. (2010) ErbB3/HER3 intracellular domain is competent to bind ATP and catalyze autophosphorylation. Proc. Natl. Acad. Sci. U.S.A. **107**, 7692–7697

20 Ungureanu, D., Wu, J., Pekkala, T., Niranjan, Y., Young, C., Jensen, O. N., Xu, C. F., Neubert, T. A., Skoda, R. C., Hubbard, S. R. and Silvennoinen, O. (2011) The pseudokinase domain of JAK2 is a dual-specificity protein kinase that negatively regulates cytokine signaling. Nat. Struct. Mol. Biol. **18**, 971–976

21 Yoshida-Moriguchi, T., Willer, T., Anderson, M. E., Venzke, D., Whyte, T., Muntoni, F., Lee, H., Nelson, S. F., Yu, L. and Campbell, K. P. (2013) SGK196 is a glycosylation-specific O-mannose kinase required for dystroglycan function. Science **341**, 896–899

22 Lucet, I. S., Babon, J. J. and Murphy, J. M. (2013) Techniques to examine nucleotide binding by pseudokinases. Biochem. Soc. Trans. **41**, 974–980

23 Stewart, R. C., VanBruggen, R., Ellefson, D. D. and Wolfe, A. J. (1998) TNP-ATP and TNP-ADP as probes of the nucleotide binding site of CheA, the histidine protein kinase in the chemotaxis signal transduction pathway of *Escherichia coli*. Biochemistry **37**, 12269–12279

24 Murphy, J. M., Metcalf, D., Young, I. G. and Hilton, D. J. (2010) A convenient method for preparation of an engineered mouse interleukin-3 analog with high solubility and wild-type bioactivity. Growth Factors **28**, 104–110

25 Babon, J. J. and Murphy, J. M. (2013) *In vitro* JAK kinase activity and inhibition assays. Methods Mol. Biol. **967**, 39–55

26 Lucet, I. S. and Bamert, R. (2013) Production and crystallization of recombinant JAK proteins. Methods Mol. Biol. **967**, 275–300

27 Fukuda, K., Gupta, S., Chen, K., Wu, C. and Qin, J. (2009) The pseudoactive site of ILK is essential for its binding to α-Parvin and localization to focal adhesions. Mol. Cell **36**, 819–830

28 Gee, C. L., Papavinasasundaram, K. G., Blair, S. R., Baer, C. E., Falick, A. M., King, D. S., Griffin, J. E., Venghatakrishnan, H., Zukauskas, A., Wei, J. R. et al. (2012) A phosphorylated pseudokinase complex controls cell wall synthesis in mycobacteria. Sci. Signaling **5**, ra7

29 Reese, M. L. and Boothroyd, J. C. (2011) A conserved non-canonical motif in the pseudoactive site of the ROP5 pseudokinase domain mediates its effect on *Toxoplasma* virulence. J. Biol. Chem. **286**, 29366–29375

30 Zeqiraj, E., Filippi, B. M., Goldie, S., Navratilova, I., Boudeau, J., Deak, M., Alessi, D. R. and van Aalten, D. M. (2009) ATP and MO25α regulate the conformational state of the STRADα pseudokinase and activation of the LKB1 tumour suppressor. PLoS Biol. **7**, e1000126

31 Bantscheff, M., Eberhard, D., Abraham, Y., Bastuck, S., Boesche, M., Hobson, S., Mathieson, T., Perrin, J., Raida, M., Rau, C. et al. (2007) Quantitative chemical proteomics reveals mechanisms of action of clinical ABL kinase inhibitors. Nat. Biotechnol. **25**, 1035–1044

32 Daub, H., Olsen, J. V., Bairlein, M., Gnad, F., Oppermann, F. S., Korner, R., Greff, Z., Keri, G., Stemmann, O. and Mann, M. (2008) Kinase-selective enrichment enables quantitative phosphoproteomics of the kinome across the cell cycle. Mol. Cell **31**, 438–448

33 Bicocca, V. T., Chang, B. H., Masouleh, B. K., Muschen, M., Loriaux, M. M., Druker, B. J. and Tyner, J. W. (2012) Crosstalk between ROR1 and the pre-B cell receptor promotes survival of t(1;19) acute lymphoblastic leukemia. Cancer Cell **22**, 656–667

34 Gentile, A., Lazzari, L., Benvenuti, S., Trusolino, L. and Comoglio, P. M. (2011) Ror1 is a pseudokinase that is crucial for Met-driven tumorigenesis. Cancer Res. **71**, 3132–3141

35 Suijkerbuijk, S. J., van Dam, T. J., Karagoz, G. E., von Castelmur, E., Hubner, N. C., Duarte, A. M., Vleugel, M., Perrakis, A., Rudiger, S. G., Snel, B. and Kops, G. J. (2012) The vertebrate mitotic checkpoint protein BUBR1 is an unusual pseudokinase. Dev. Cell **22**, 1321–1329

36 Hovens, C. M., Stacker, S. A., Andres, A. C., Harpur, A. G., Ziemiecki, A. and Wilks, A. F. (1992) RYK, a receptor tyrosine kinase-related molecule with unusual kinase domain motifs. Proc. Natl. Acad. Sci. U.S.A. **89**, 11818–11822

37 Nimchuk, Z. L., Tarr, P. T. and Meyerowitz, E. M. (2011) An evolutionarily conserved pseudokinase mediates stem cell production in plants. Plant Cell **23**, 851–854

38 Kim, J. G., Li, X., Roden, J. A., Taylor, K. W., Aakre, C. D., Su, B., Lalonde, S., Kirik, A., Chen, Y., Baranage, G. et al. (2009) *Xanthomonas* T3S effector XopN suppresses PAMP-triggered immunity and interacts with a tomato atypical receptor-like kinase and TFT1. Plant Cell **21**, 1305–1323

39 Labesse, G., Gelin, M., Bessin, Y., Lebrun, M., Papoin, J., Cerdan, R., Arold, S. T. and Dubremetz, J. F. (2009) ROP2 from *Toxoplasma gondii*: a virulence factor with a protein-kinase fold and no enzymatic activity. Structure **17**, 139–146

40 Buchholz, K. R., Bowyer, P. W. and Boothroyd, J. C. (2013) Bradyzoite pseudokinase 1 is crucial for efficient oral infectivity of the *Toxoplasma* tissue cyst. Eukaryotic Cell **12**, 399–410

41 Fukuda, K., Knight, J. D., Piszczek, G., Kothary, R. and Qin, J. (2011) Biochemical, proteomic, structural, and thermodynamic characterizations of integrin-linked kinase (ILK): cross-validation of the pseudokinase. J. Biol. Chem. **286**, 21886–21895

42 Lo, M. C., Aulabaugh, A., Jin, G., Cowling, R., Bard, J., Malamas, M. and Ellestad, G. (2004) Evaluation of fluorescence-based thermal shift assays for hit identification in drug discovery. Anal. Biochem. **332**, 153–159

43 Murphy, J. M., Czabotar, P. E., Hildebrand, J. M., Lucet, I. S., Zhang, J. G., Alvarez-Diaz, S., Lewis, R., Lalaoui, N., Metcalf, D., Webb, A. I. et al. (2013) The pseudokinase MLKL mediates necroptosis via a molecular switch mechanism. Immunity **39**, 443–453

44 Bullock, A. N., Debreczeni, J. E., Fedorov, O. Y., Nelson, A., Marsden, B. D. and Knapp, S. (2005) Structural basis of inhibitor specificity of the human protooncogene proviral insertion site in Moloney murine leukemia virus (PIM-1) kinase. J. Med. Chem. **48**, 7604–7614

45 Babon, J. J., Kershaw, N. J., Murphy, J. M., Varghese, L. N., Laktyushin, A., Young, S. N., Lucet, I. S., Norton, R. S. and Nicola, N. A. (2012) Suppression of cytokine signaling by SOCS3: characterization of the mode of inhibition and the basis of its specificity. Immunity **36**, 239–250

46 Becher, I., Savitski, M. M., Savitski, M. F., Hopf, C., Bantscheff, M. and Drewes, G. (2013) Affinity profiling of the cellular kinome for the nucleotide cofactors ATP, ADP, and GTP. ACS Chem. Biol. **8**, 599–607

47 Kang, J., Yang, M., Li, B., Qi, W., Zhang, C., Shokat, K. M., Tomchick, D. R., Machius, M. and Yu, H. (2008) Structure and substrate recruitment of the human spindle checkpoint kinase Bub1. Mol. Cell **32**, 394–405

48 Baxter, E. J., Scott, L. M., Campbell, P. J., East, C., Fourouclas, N., Swanton, S., Vassiliou, G. S., Bench, A. J., Boyd, E. M., Curtin, N. et al. (2005) Acquired mutation of the tyrosine kinase JAK2 in human myeloproliferative disorders. Lancet **365**, 1054–1061

49 James, C., Ugo, V., Le Couedic, J. P., Staerk, J., Delhommeau, F., Lacout, C., Garcon, L., Raslova, H., Berger, R., Bennaceur-Griscelli, A. et al. (2005) A unique clonal JAK2 mutation leading to constitutive signalling causes polycythaemia vera. Nature **434**, 1144–1148

50 Kralovics, R., Passamonti, F., Buser, A. S., Teo, S. S., Tiedt, R., Passweg, J. R., Tichelli, A., Cazzola, M. and Skoda, R. C. (2005) A gain-of-function mutation of JAK2 in myeloproliferative disorders. N. Engl. J. Med. **352**, 1779–1790

51 Levine, R. L., Wadleigh, M., Cools, J., Ebert, B. L., Wernig, G., Huntly, B. J., Boggon, T. J., Wlodarska, I., Clark, J. J., Moore, S. et al. (2005) Activating mutation in the tyrosine kinase JAK2 in polycythemia vera, essential thrombocythemia, and myeloid metaplasia with myelofibrosis. Cancer Cell **7**, 387–397

52 Zhao, R., Xing, S., Li, Z., Fu, X., Li, Q., Krantz, S. B. and Zhao, Z. J. (2005) Identification of an acquired JAK2 mutation in polycythemia vera. J. Biol. Chem. **280**, 22788–22792

53 Bandaranayake, R. M., Ungureanu, D., Shan, Y., Shaw, D. E., Silvennoinen, O. and Hubbard, S. R. (2012) Crystal structures of the JAK2 pseudokinase domain and the pathogenic mutant V617F. Nat. Struct. Mol. Biol. **19**, 754–759

54 Zeqiraj, E., Filippi, B. M., Deak, M., Alessi, D. R. and van Aalten, D. M. (2009) Structure of the LKB1–STRAD–MO25 complex reveals an allosteric mechanism of kinase activation. Science **326**, 1707–1711

55 Artim, S. C., Mendrola, J. M. and Lemmon, M. A. (2012) Assessing the range of kinase autoinhibition mechanisms in the insulin receptor family. Biochem. J. **448**, 213–220

56 Jung, J. W., Shin, W. S., Song, J. and Lee, S. T. (2004) Cloning and characterization of the full-length mouse *Ptk7* cDNA encoding a defective receptor protein tyrosine kinase. Gene **328**, 75–84
57 Wesche, H., Gao, X., Li, X., Kirschning, C. J., Stark, G. R. and Cao, Z. (1999) IRAK-M is a novel member of the Pelle/interleukin-1 receptor-associated kinase (IRAK) family. J. Biol. Chem. **274**, 19403–19410
58 Gurniak, C. B. and Berg, L. J. (1996) A new member of the Eph family of receptors that lacks protein tyrosine kinase activity. Oncogene **13**, 777–786
59 Matsuoka, H., Iwata, N., Ito, M., Shimoyama, M., Nagata, A., Chihara, K., Takai, S. and Matsui, T. (1997) Expression of a kinase-defective Eph-like receptor in the normal human brain. Biochem. Biophys. Res. Commun. **235**, 487–492
60 Zhao, J., Jitkaew, S., Cai, Z., Choksi, S., Li, Q., Luo, J. and Liu, Z. G. (2012) Mixed lineage kinase domain-like is a key receptor interacting protein 3 downstream component of TNF-induced necrosis. Proc. Natl. Acad. Sci. U.S.A. **109**, 5322–5327
61 Carrera, A. C., Alexandrov, K. and Roberts, T. M. (1993) The conserved lysine of the catalytic domain of protein kinases is actively involved in the phosphotransfer reaction and not required for anchoring ATP. Proc. Natl. Acad. Sci. U.S.A. **90**, 442–446
62 Murphy, J. M., Lucet, I. S., Hildebrand, J. M., Tanzer, M. C., Young, S. N., Sharma, P., Lessene, G., Alexander, W. S., Babon, J. J., Silke, J. and Czabotar, P. E. (2013) Insights into the evolution of divergent nucleotide-binding mechanisms among pseudokinases revealed by crystal structures of human and mouse MLKL. Biochem. J., doi:10.1042/BJ20131270
63 Jaleel, M., Saha, S., Shenoy, A. R. and Visweswariah, S. S. (2006) The kinase homology domain of receptor guanylyl cyclase C: ATP binding and identification of an adenine nucleotide sensitive site. Biochemistry **45**, 1888–1898
64 Kelber, J. A., Reno, T., Kaushal, S., Metildi, C., Wright, T., Stoletov, K., Weems, J. M., Park, F. D., Mose, E., Wang, Y. et al. (2012) KRas induces a Src/PEAK1/ErbB2 kinase amplification loop that drives metastatic growth and therapy resistance in pancreatic cancer. Cancer Res. **72**, 2554–2564
65 Wang, Y., Kelber, J. A., Tran Cao, H. S., Cantin, G. T., Lin, R., Wang, W., Kaushal, S., Bristow, J. M., Edgington, T. S., Hoffman, R. M. et al. (2010) Pseudopodium-enriched atypical kinase 1 regulates the cytoskeleton and cancer progression. Proc. Natl. Acad. Sci. U.S.A. **107**, 10920–10925
66 Kawagoe, T., Sato, S., Matsushita, K., Kato, H., Matsui, K., Kumagai, Y., Saitoh, T., Kawai, T., Takeuchi, O. and Akira, S. (2008) Sequential control of Toll-like receptor-dependent responses by IRAK1 and IRAK2. Nat. Immunol. **9**, 684–691
67 Pauls, E., Nanda, S. K., Smith, H., Toth, R., Arthur, J. S. and Cohen, P. (2013) Two phases of inflammatory mediator production defined by the study of IRAK2 and IRAK1 knock-in mice. J. Immunol. **191**, 2717–2730
68 Lange, A., Wickstrom, S. A., Jakobson, M., Zent, R., Sainio, K. and Fassler, R. (2009) Integrin-linked kinase is an adaptor with essential functions during mouse development. Nature **461**, 1002–1006
69 Mendrola, J. M., Shi, F., Park, J. H. and Lemmon, M. A. (2013) Receptor tyrosine kinases with intracellular pseudokinase domains. Biochem. Soc. Trans. **41**, 1029–1036
70 Toms, A. V., Deshpande, A., McNally, R., Jeong, Y., Rogers, J. M., Kim, C. U., Gruner, S. M., Ficarro, S. B., Marto, J. A., Sattler, M. et al. (2013) Structure of a pseudokinase-domain switch that controls oncogenic activation of Jak kinases. Nat. Struct. Mol. Biol. **20**, 1221–1223
71 Huse, M. and Kuriyan, J. (2002) The conformational plasticity of protein kinases. Cell **109**, 275–282
72 Zeqiraj, E. and van Aalten, D. M. (2010) Pseudokinases: remnants of evolution or key allosteric regulators? Curr. Opin. Struct. Biol. **20**, 772–781
73 Kannan, N., Taylor, S. S., Zhai, Y., Venter, J. C. and Manning, G. (2007) Structural and functional diversity of the microbial kinome. PLoS Biol. **5**, e17

Received 30 August 2013/8 October 2013; accepted 10 October 2013
Published as BJ Immediate Publication 10 October 2013, doi:10.1042/BJ20131174

Biochem. J. (2014) **457**, 323–334 (Printed in Great Britain) doi:10.1042/BJ20131174

online data

SUPPLEMENTARY ONLINE DATA

A robust methodology to subclassify pseudokinases based on their nucleotide-binding properties

James M. MURPHY*†[1,2], Qingwei ZHANG‡, Samuel N. YOUNG*, Michael L. REESE§[3], Fiona P. BAILEY¶, Patrick A. EYERS¶, Daniela UNGUREANU‖, Henrik HAMMAREN‖, Olli SILVENNOINEN‖, Leila N. VARGHESE*†, Kelan CHEN*†, Anne TRIPAYDONIS*, Natalia JURA**, Koichi FUKUDA††, Jun QIN††, Zachary NIMCHUK‡‡[4], Mary Beth MUDGETT§§, Sabine ELOWE¶¶, Christine L. GEE‖‖, Ling LIU***[5], Roger J. DALY***[5], Gerard MANNING†††, Jeffrey J. BABON*† and Isabelle S. LUCET‡[1,2]

*The Walter and Eliza Hall Institute of Medical Research, Parkville, Victoria 3052, Australia
†Department of Medical Biology, University of Melbourne, Parkville, Victoria 3050, Australia
‡Department of Biochemistry and Molecular Biology, School of Biomedical Sciences, Monash University, Clayton, Victoria 3800, Australia
§Department of Microbiology and Immunology, Stanford University, Stanford, CA 24305-5124, U.S.A.
¶Department of Biochemistry, Institute of Integrative Biology, University of Liverpool, Liverpool L69 7ZB, U.K.
‖School of Medicine and Institute of Biomedical Technology, University of Tampere and Tampere University Hospital, Tampere 33014, Finland
**Cardiovascular Research Institute and Department of Cellular and Molecular Pharmacology, University of California San Francisco, San Francisco, CA 94158-9001, U.S.A.
††Department of Molecular Cardiology, Lerner Research Institute, NB20, Cleveland Clinic, 9500 Euclid Avenue, Cleveland, OH 44195, U.S.A.
‡‡Department of Biology, California Institute of Technology, Pasadena, CA 91125, U.S.A.
§§Department of Biology, Stanford University, Stanford, CA 24305-5020, U.S.A.
¶¶Centre de Recherche du Centre Hospitalier Universitaire de Québec and and Faculté de Médicine, Département de Pédiatrie, Université Laval, Québec G1V 4G2, Canada
‖‖Australian Synchrotron, Clayton, Victoria 3168, Australia
***Cancer Research Program, The Kinghorn Cancer Centre, Garvan Institute of Medical Research, 370 Victoria Street, Darlinghurst, Sydney, NSW 2010, Australia
†††Genentech, 1 DNA Way, MS 93, South San Francisco, CA 94010, U.S.A.

Supplementary Figures S1–S3 and Supplementary Table S1 are on the following pages.

[1] These authors contributed equally to this work.
[2] Correspondence may be addressed to either of these authors (email jamesm@wehi.edu.au or isabelle.lucet@monash.edu).
[3] Present address: Department of Pharmacology, University of Texas, Southwestern Medical Center, 6001 Forest Park Road, Dallas, TX 75390-9041, U.S.A.
[4] Present address: Department of Biological Sciences, Virginia Tech, 220 Ag Quad Lane, Blacksburg, VA 24061, U.S.A.
[5] Present address: Department of Biochemistry and Molecular Biology, School of Biomedical Sciences, Monash University, Clayton, Victoria 3800, Australia.

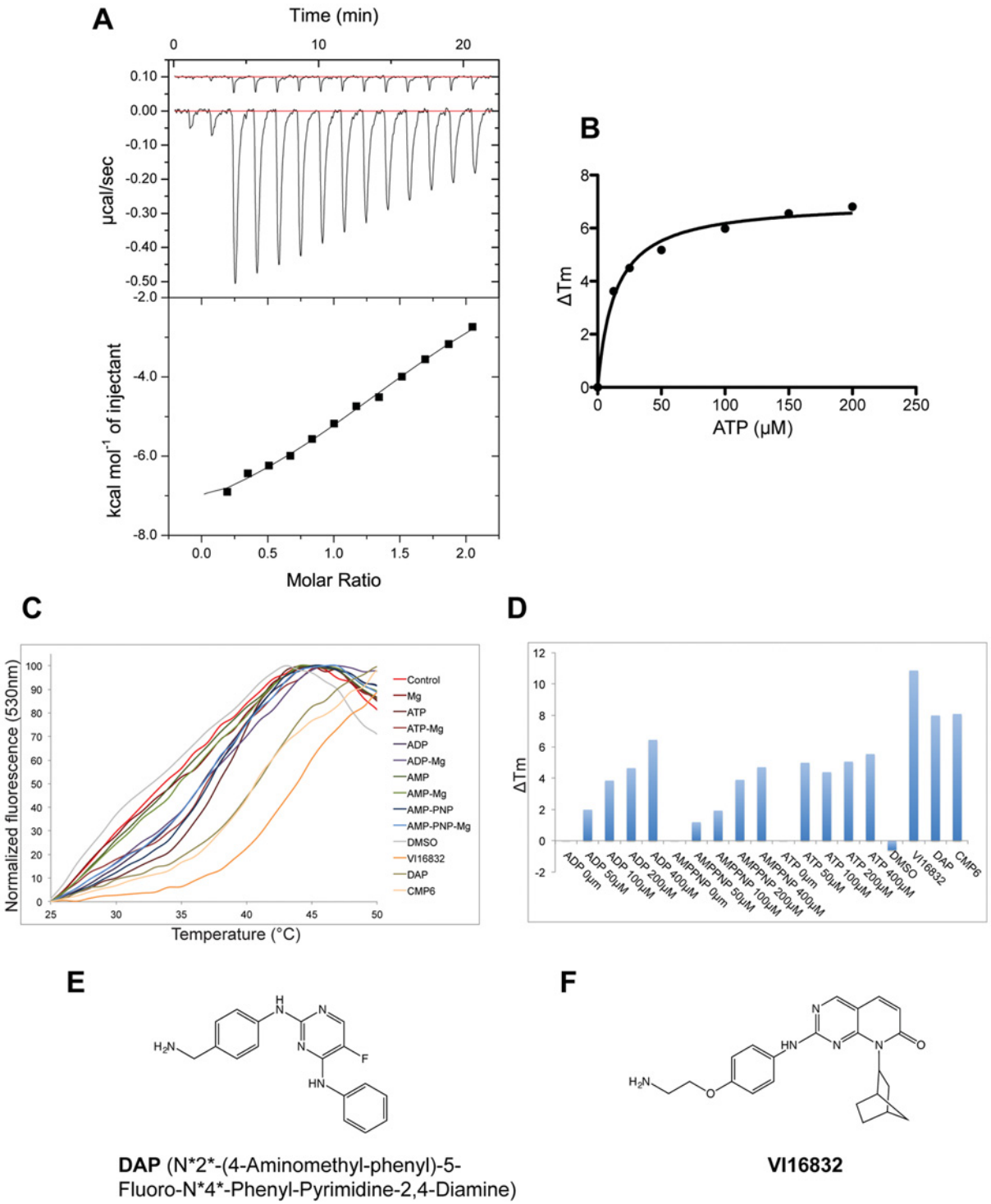

Figure S1 Validation of the thermal-shift assay for detecting ligand binding

(**A**) ITC data demonstrating ATP binding to MLKL. Upper panel: the upper isotherm represents a buffer control and the lower isotherm represents the injection and binding of ATP to 50 μM MLKL. The K_d value for the experiment shown was calculated as 20 μM. The K_d value calculated from a second experiment (results not shown) was 15 μM. (**B**) Titration of MLKL with increasing concentrations of ATP in the thermal-shift assay. The data from two independent experiments yielded a K_d value (mean$\pm$S.E.M.) of 13.6$\pm$1.9 μM. (**C**) Thermal denaturation curves for the tyrosine kinase (JH1) domain of JAK2 in the presence of 200 μM nucleotide in the presence or absence of 1 mM Mg^{2+}. The inhibitors VI16832 and DAP, as well as the JAK-specific inhibitor CMP6, all at concentrations of 40 μM, were included as positive controls. (**D**) ΔT_m analyses of JAK2(JH1) nucleotide-binding titrations (0–400 μM nucleotide concentration) in the presence of 1 mM Mg^{2+}. At a 200 μM nucleotide concentration (the concentration used elsewhere in the present study), we could detect ADP, ATP and AMP-PNP binding to JAK2(JH1), consistent with a limit of detection corresponding to K_d values in excess of 200 μM. (**E** and **F**) Chemical structures of the promiscuous inhibitors DAP [5] (**E**) and VI16832 [6,7] (**F**).

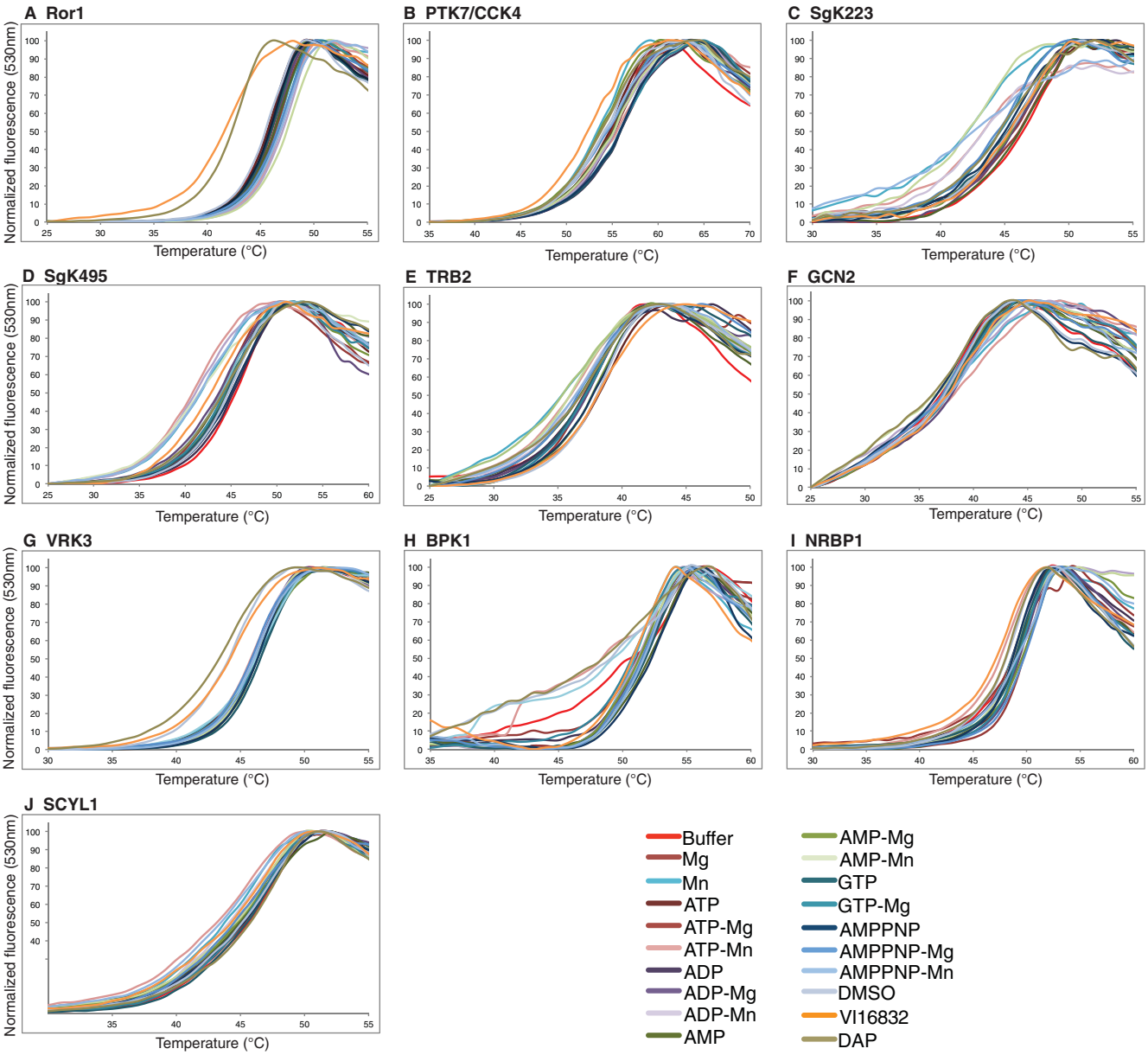

Figure S2 Thermal denaturation curves of Class 1 (no detectable nucleotide or cation binding) pseudokinases

Selected data from this pseudokinase subclass are presented in Figure 2 of the main text. Thermal denaturation curves for Ror1 (**A**), PTK7/CCK4 (**B**), SgK223 (**C**), SgK495 (**D**), TRB2 (**E**), GCN2 (**F**), VRK3 (**G**), BPK1 (**H**), NRBP1 (**I**) and SCYL1 [SCY1-like 1 (*S. cerevisiae*)] (**J**) did not detectably shift in the presence of nucleotides with or without cations. A colour key for the curve labelling is underneath the curves. Control experiments establishing sensitivity of the assay for nucleotide binding are shown in Figure S1.

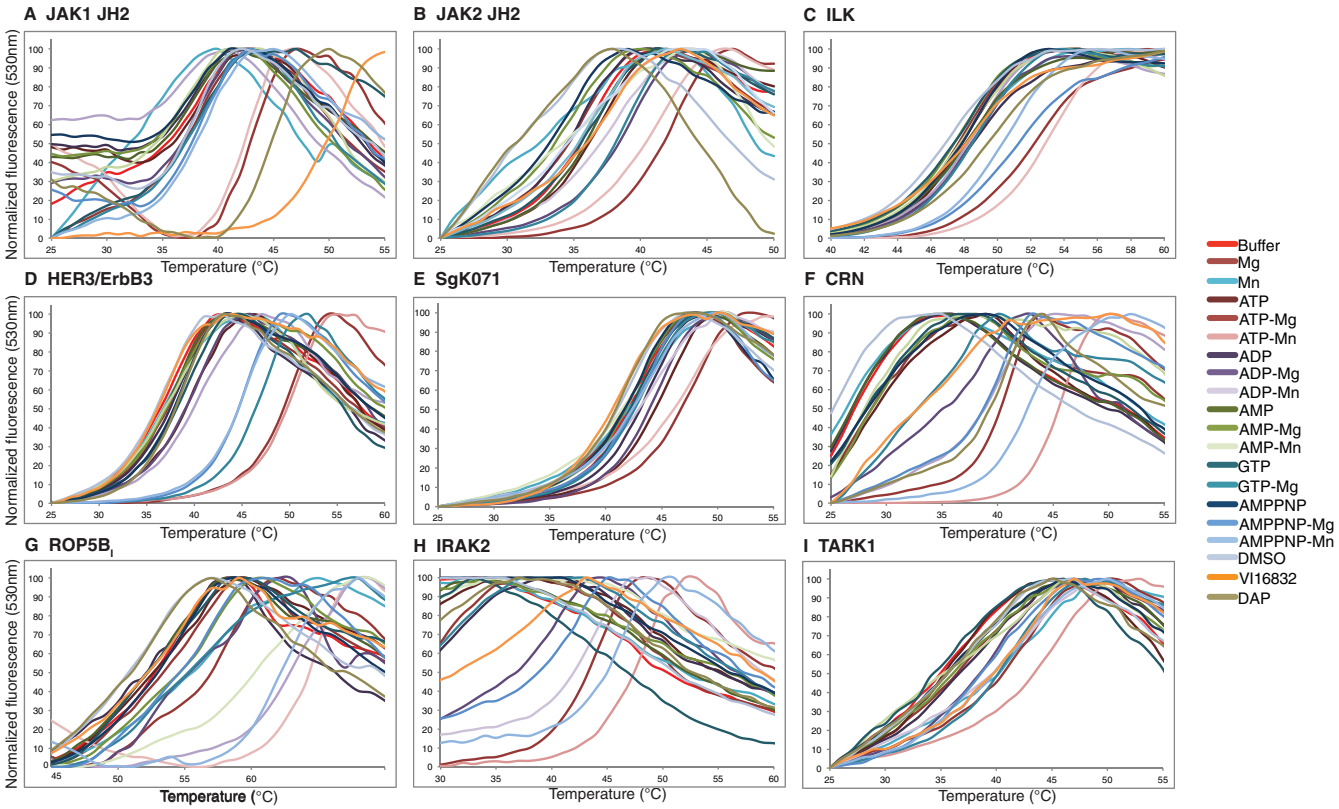

Figure S3 Thermal denaturation curves of Class 4 (nucleotide- and cation-binding) pseudokinases

The ΔT_m values calculated from these curves are presented as histograms in Figure 4 of the main text.

Table S1 Sources of cDNA templates for previously undescribed expression constructs

Gene	GenBank® accession number	Template source	Reference
PTK7/CCK4	U40271	Professor S.-T. Lee	[1]
Ror1	NM_005012	Dr A. Gentile	[2]
IRAK3	NM_007199	Dr William Hahn* via Addgene (plasmid 23627)	[3]
GCN2	BC072637	IMAGE clone 30354433	
ULK4	NM_017886	Dr William Hahn* via Addgene (plasmid 23849)	[3]
IRAK2	NM_001570	Dr William Hahn* via Addgene (plasmid 23412)	[3]
MLKL	NM_152649	Synthetic; DNA2.0 (CA)	
VRK3	BC095449	IMAGE clone 30721912	
TARK1	FJ176293	M.B. Mudgett	[4]
EphB6	NM_004445	Dr William Hahn* via Addgene (plasmid 23931)	[3]
NRBP1	NM_013392	Dr William Hahn* via Addgene (plasmid 23568)	[3]
SCYL1	BC069233	IMAGE clone 6581110	
RYK	BC032275	IMAGE clone 5370100	
CASK	NM_003688	IMAGE clone 40125862	
SgK495/STK40	NM_032017	IMAGE clone 4109652	
TRB2	BC002637	IMAGE clone 3607549	
SgK071/C9orf96	NM_153710	IMAGE clone 5265506	

*Harvard Medical School, Boston, MA, U.S.A.

REFERENCES

1 Park, S. K., Lee, H. S. and Lee, S. T. (1996) Characterization of the human full-length PTK7 cDNA encoding a receptor protein tyrosine kinase-like molecule closely related to chick KLG. J. Biochem. **119**, 235–239

2 Gentile, A., Lazzari, L., Benvenuti, S., Trusolino, L. and Comoglio, P. M. (2011) Ror1 is a pseudokinase that is crucial for Met-driven tumorigenesis. Cancer Res. **71**, 3132–3141

3 Johannessen, C. M., Boehm, J. S., Kim, S. Y., Thomas, S. R., Wardwell, L., Johnson, L. A., Emery, C. M., Stransky, N., Cogdill, A. P., Barretina, J. et al. (2010) COT drives resistance to RAF inhibition through MAP kinase pathway reactivation. Nature **468**, 968–972

4 Kim, J. G., Li, X., Roden, J. A., Taylor, K. W., Aakre, C. D., Su, B., Lalonde, S., Kirik, A., Chen, Y., Baranage, G. et al. (2009) *Xanthomonas* T3S effector XopN suppresses PAMP-triggered immunity and interacts with a tomato atypical receptor-like kinase and TFT1. Plant Cell **21**, 1305–1323

5 Bantscheff, M., Eberhard, D., Abraham, Y., Bastuck, S., Boesche, M., Hobson, S., Mathieson, T., Perrin, J., Raida, M., Rau, C. et al. (2007) Quantitative chemical proteomics reveals mechanisms of action of clinical ABL kinase inhibitors. Nat. Biotechnol. **25**, 1035–1044

6 Daub, H., Olsen, J. V., Bairlein, M., Gnad, F., Oppermann, F. S., Korner, R., Greff, Z., Keri, G., Stemmann, O. and Mann, M. (2008) Kinase-selective enrichment enables quantitative phosphoproteomics of the kinome across the cell cycle. Mol. Cell **31**, 438–448

7 Oppermann, F. S., Gnad, F., Olsen, J. V., Hornberger, R., Greff, Z., Keri, G., Mann, M. and Daub, H. (2009) Large-scale proteomics analysis of the human kinome. Mol. Cell. Proteomics **8**, 1751–1764

Received 30 August 2013/8 October 2013; accepted 10 October 2013
Published as BJ Immediate Publication 10 October 2013, doi:10.1042/BJ20131174